Available online at www.sciencedirect.com
SCIENCE DIRECT®
Journal of Magnetic Resonance 171 (2004) 353–358
JMR Journal of Magnetic Resonance
www.elsevier.com/locate/jmr

Communication

An open volume, high isolation, radio frequency surface coil system for pulsed magnetic resonance

Carlo Alberto Curto[a], Giuseppe Placidi[b], Antonello Sotgiu[a], Marcello Alecci[a,*]

[a] *INFM and Dipartimento di Scienze e Tecnologie Biomediche, Università dell'Aquila, Via Vetoio, 67100 L'Aquila, Italy*
[b] *INFM and Centro di Risonanza Magnetica, Università dell'Aquila, 67100 L'Aquila, Italy*

Received 13 March 2004; revised 25 August 2004
Available online 14 October 2004

Abstract

We present an open volume, high isolation, RF system suitable for pulsed NMR and EPR spectrometers with reduced dead time. It comprises a set of three RF surface coils disposed with mutually parallel RF fields and a double-channel receiver (RX). Theoretical and experimental results obtained with a prototype operating at about 100 MHz are reported. Each surface RF coil (diameter 5.5 cm) was tuned to $f_0 = 100.00 \pm 0.01$ MHz when isolated. Because of the mutual coupling and the geometry of the RF coils, only two resonances at $f_1 = 97.94$ MHz and $f_2 = 101.85$ MHz were observed. We show they are associated with two different RF field spatial distributions. In continuous mode (CW) operation the isolation between the TX coil and one of the RX coils (single-channel) was about -10 dB. By setting the double-channel RF assembly in subtraction mode the isolation values at f_1 or f_2 could be optimised to about -75 dB. Following a TX RF pulse (5 μs duration) an exponential decay with time constant of about 600 ns was observed. The isolation with single-channel RX coil was about -11 dB and it increased to about -47 dB with the double-channel RX in subtraction mode. Similar results were obtained with the RF pulse frequency selected to f_2 and also with shorter (500 ns) RF pulses. The above geometrical parameters and operating frequency of the RF assembly were selected as a model for potential applications in solid state NMR and in free radical EPR spectroscopy and imaging.
© 2004 Elsevier Inc. All rights reserved.

Keywords: RF coil; Dead time; NMR; EPR; Imaging

1. Introduction

In recent years there has been increasing interest in the use of NMR imaging to examine solid materials, porous media, and solvent diffusion in solids. Here restricted motion of the observed spins leads to broad lines and very-short relaxation times (100 μs or less) [1]. Continuous wave [2,3] and pulsed [4] NMR techniques have been developed to image solid state materials. However, one of the main instrumental limitations of pulsed methods is the dead time of the RF receiver. A similar problem is encountered in EPR spectroscopy and imaging of paramagnetic probes, where the relaxation times are ultra-short (10 μs or less) [5–8].

Magnetic resonance scanners capable of detecting nuclei or paramagnetic species with very-short relaxation times require a transmitter (TX) and receiver (RX) system with "zero" dead time. The practical achievement of this condition depends mainly on the overall isolation between TX and RX RF coils. Over the past years, several solutions for increasing the isolation have been developed [9–12]. Recently, a submicrosecond RF system equipped with a single TX *volume* RF coil and a RX made of two *volume* RF coils has been presented [5,13,14]. It was shown that in the presence of "weakly" coupled RF volume coils the isolation increases significantly as the tuning frequency offset, with respect to

* Corresponding author. Fax:+39 0862 433433.
E-mail addresses: marcello.alecci@univaq.it, alecci@fismedw2.univaq.it (M. Alecci).

1090-7807/$ - see front matter © 2004 Elsevier Inc. All rights reserved.
doi:10.1016/j.jmr.2004.09.015

the Larmor frequency f_0, between the TX and RX coils decreases [15].

In the previous systems, the TX/RX volume coils were geometrically arranged to produce RF fields in mutually perpendicular directions and the RX coils surrounded the object under study. Moreover, the two RX coils were aligned to produce RF fields perpendicular to each other, and with the RF field of one of the RX coils parallel to the static magnetic field B_0. This design is effective for reducing the dead time [5,13–15], but poses some limitations for the RF coil design and also for the easy access of the sample under study. These constrains can be particularly demanding if the apparatus is intended for in vivo EPR imaging. We have recently described a novel open volume RF system that allows high isolation between the TX and RX coils [16]. The RF system is made by a set of three RF *surface* coils that can be positioned with mutually perpendicular or mutually parallel RF fields. A preliminary description of one embodiment of the apparatus made by three perpendicular RF surface coils was presented [17].

In this work, we describe the design and testing of an open volume, high isolation, TX/RX system equipped with RF surface coils. We have studied a configuration comprising three RF circular loop coils with mutually parallel RF fields. Theoretical and experimental data of a prototype operating at about 100 MHz are reported.

2. Methods and results

2.1. Design of the RF assembly with parallel coils

Fig. 1 shows a prototype of the RF system composed by three RF surface coils geometrically positioned to be parallel to each other. The circular loop RF coil geometry was chosen for easy of operation; however the RF system would be effective with arbitrary RF coil geometry (e.g., square or rectangular loop). As shown in Fig. 1, this open volume configuration allows the sample to be easily positioned between the TX RF coil (middle) and one of the RX RF coil (side). With the current prototype the center-to-center distance (d_{cc}) between each pair of RF coils was 6.0 cm.

The RF assembly is made by three "identical" circular RF coils (diameter of 5.5 cm) made of adhesive copper tape (width 5 mm, thickness 150 μm). Each RF coil has a measured inductance L of about 0.10 μH and this value is in reasonable agreement with theory ($L = 0.13$ μH) [18]. A non-magnetic trimmer capacitor C_T (1–16 pF) was used for tuning each RF coil at about 100 MHz. As shown in Fig. 2, a balanced capacitive matching circuit [19] made of chip capacitors ($C_1 = 22$ pF, $C_M = 200$ pF) was used for impedance matching. To achieve a fine matching adjustment a trimmer capacitor (not shown in Fig. 2) of value 1–16 pF was connected in parallel with the chip capacitor C_M.

Fig. 1. Prototype of the RF system made of three parallel circular loop RF surface coils. The center-to-center distance (d_{cc}) between each pair of RF coils was 6.0 cm. Each coil (diameter 5.5 cm) was built on a Plexiglas substrate and was made of adhesive copper tape (width 5 mm, thickness 150 μm). A trimmer capacitor (1–16 pF) was connected for tuning the RF coil at $f_0 = 100.00 \pm 0.01$ MHz when isolated. A capacitive balanced network was used for impedance matching [19]. A BNC coaxial connector was mounted on the Plexiglas substrate and used for connecting the coil to the RX via a 50 Ω coaxial cable (RG58). The measured quality factor Q was 132 when empty and it decreased to 110 in the presence of a phantom containing 500 ml of physiological saline solution.

The above geometrical parameters (loop diameter and d_{cc}) and operating frequency (100 MHz) were selected, in the present work, as a reference model for potential applications of the RF assembly in solid state NMR and in vivo EPR spectroscopy/imaging. However, we anticipate that this RF assembly design should be suited for a broader range of geometrical dimensions and operating frequencies.

Fig. 2 shows schematically the RF assembly comprising a set of three RF surface coils and the double-channel RX system. This design has been previously described [13,14], however the apparatus presented here is characterised by the following new features: (i) it allows the use of RF surface coils; (ii) it allows an open volume access for the sample; (iii) it allows to operate with "strongly" coupled RF coils; and (iv) it achieves high isolation between the TX and RX at the Larmor frequency, i.e., a significant reduction of the dead time. In particular, the design features of the RF assembly are: (a) use of separate TX and RX coils (crossed configuration), with both the TX and RX coils tuned to $f_0 = 100.00 \pm 0.01$ MHz when isolated; (b) use of a TX RF surface coil, having the RF field in a direction perpendicular to the main magnetic field B_0; (c) use of a RX system composed of two RF surface coils (RX_S and RX_R), both tuned to f_0 when isolated and with

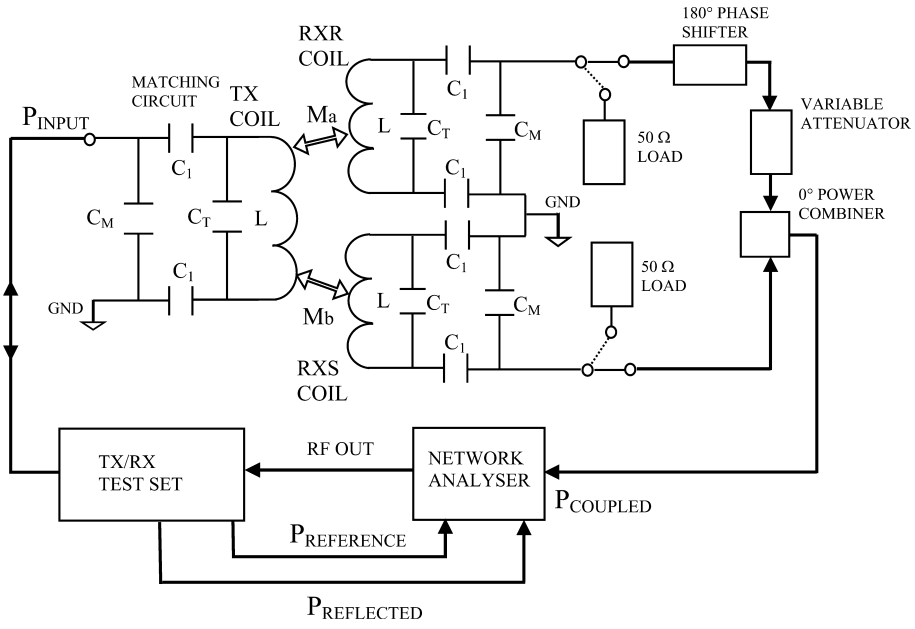

Fig. 2. Schematic design of the double-channel RF assembly comprising a TX RF surface coil, two RX RF surface coils (RX_S and RX_R), a variable attenuator (HP 355C), a homebuilt phase shifter, a 0° power combiner (Mini Circuits, ZFSCJ 1-4). A network analyser (HP 8753A) and a TX/RX test set (HP85044A) were used to measure the S_{11} (reflection) and S_{21} (isolation) scattering parameters of the RF assembly. The S_{21} was measured between the TX coil and the: (i) RX_S (or RX_R) coil alone; (ii) RX_S coil in the presence of the RX_R coil (with the RX_R coil connected to a 50 Ω load) and vice versa; and (iii) output of the power combiner, with the RX_S and RX_R coils in "subtraction" mode (phase shift = 180°, attenuation = 1 dB).

the same ringing time, i.e., the same quality factor Q; (d) the sample is positioned between the TX and RX_S coils; (e) the RX_S coil is accurately oriented to produce a RF field in a direction perpendicular to B_0 and is used for FID detection; (f) the RX_R coil is positioned away from the sample and is used for dead time reduction; (g) for easy of operation, the RX_R coil is oriented in a symmetric position with respect to the TX coil and the RF field is in a direction perpendicular to B_0.

Because of the finite isolation between the TX and RX coils, and taking into account the symmetry of the system, the same ringing voltages (amplitude and phase) are induced in the RX_S and RX_R coils by the RF pulses applied to the TX coil. As shown in Fig. 2, an adjustable 180° phase shifter and a variable attenuator are inserted in cascade with the RX_R coil. If the signals in the two arms of the RX system are balanced and exactly out-of-phase, a marked increase of the isolation at the output of the power combiner is observed. It is worth noting that, in some experimental conditions, the variable attenuator may be inserted in cascade with the RX_S coil to better achieve the balance of the receiver system.

2.2. S_{11} response of the RF assembly

A network analyser and a TX/RX test set were used to measure the scattering parameter S_{11} (reflected power) of the RF coils (Fig. 2). When isolated the S_{11} parameter of each of the RF coils showed a single peak centred at f_0. When the three RF coils are symmetrically positioned (Fig. 1) at a given distance d_{cc} two resonant frequencies are expected. A typical example of the S_{11} of the RF assembly, as seen by the TX RF coil, is reported in Fig. 3. It was experimentally verified the existence of two resonances at $f_1 = 97.94$ MHz and $f_2 = 101.85$ MHz. This S_{11} response can be modelled with the theory of coupled resonant circuits [20]. Because of the mutual inductance between the three RF coils, a number of resonant frequencies around f_0 should

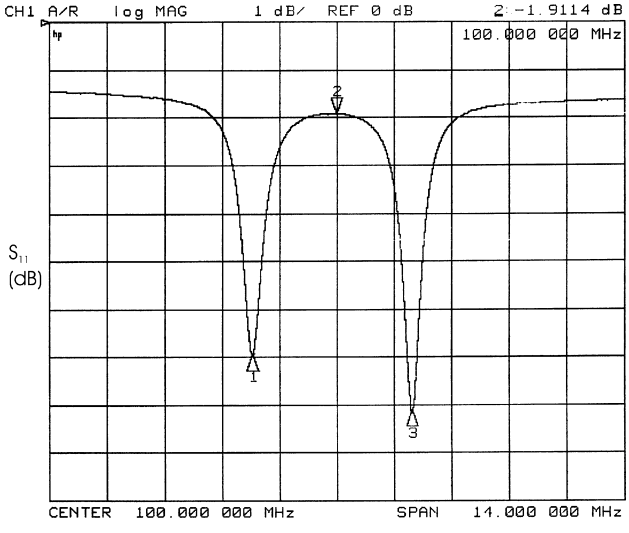

Fig. 3. Typical measured S_{11} response (reflection) of the RF assembly as seen by the TX RF coil. The resonances were at $f_1 = 97.94$ MHz and $f_2 = 101.85$ MHz.

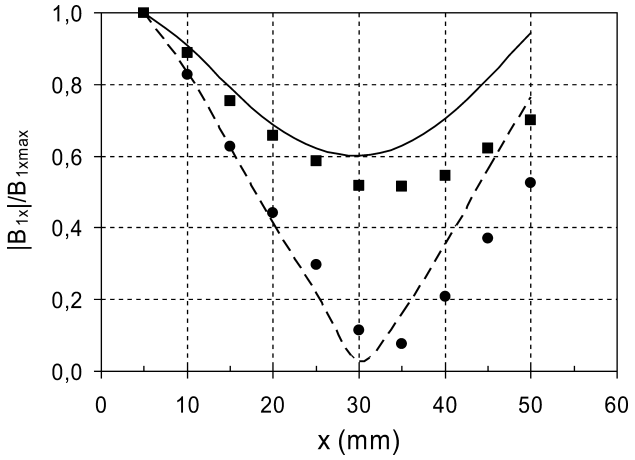

Fig. 4. Theoretical and experimental normalised RF B_{1x} field amplitude versus x-axis position for the f_1 (squares and continuous line) and f_2 (circle and dashed line) modes. The zero x-axis value corresponds to the position of the TX coil. The RF field amplitude was measured (in between the TX and RX_S coils) with a small pick-up solenoid (6 turns, diameter 4 mm, length 4 mm) built and mounted on a mechanical sliding system that allows accurate positioning (±1 mm). The RF output of the network analyser operating in CW mode was connected to the TX RF coil and the pick-up probe voltage was measured with a digital oscilloscope (HP 54502A).

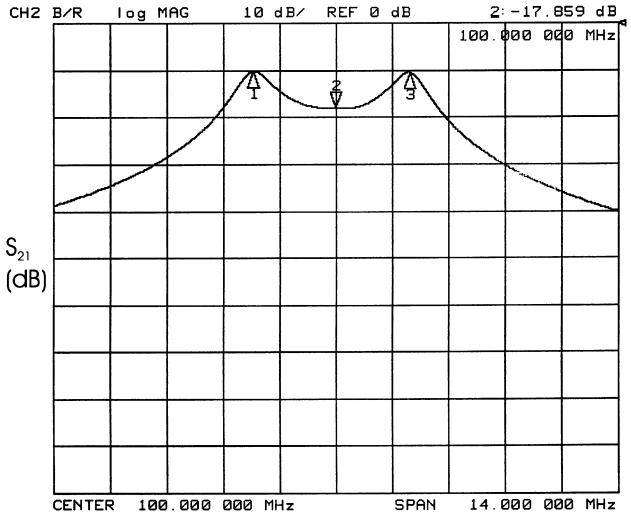

Fig. 5. Typical S_{21} response (isolation) of the RF assembly measured between the TX and RX_S coils (single channel), in the presence of the RX_R coil connected to a 50 load. The measured isolation for both peaks ($f_1 = 97.94$ MHz and $f_2 = 101.85$ MHz) was about −10 dB.

be observed. However, due to the geometrical symmetry of the RF system, only two resonant frequencies are observed. The f_1 and f_2 resonances can be associated with two different RF currents distributions which, in turn, will give two different RF field distributions [21]. We have used a numerical integration of the Biot–Savart law to simulate the three-dimensional B_1 field distributions of the RF assembly. A current of 1 A was assumed in each of the three RF coils. Experimental mapping of the RF B_1 field amplitude was obtained with the method of the pick-up probe [19].

Fig. 4 shows the theoretical and experimental B_{1x} amplitude along the RF assembly x-axis, sampled in between the TX and RX_S coils for both f_1 and f_2. A reasonable agreement between theory and experiment was observed. With the present geometry ($d_{cc} = 6.0$ cm) we found that: the f_1 mode exhibits a good RF field homogeneity, with the B_{1x} variation less than 20% in a central region of about 3.5 cm; on the contrary, the f_2 mode exhibits a large RF inhomogeneity with a minimum at about 3 cm from the TX coil. It is worth noting that the RF field distributions of the f_1 and f_2 modes make them more suitable for volume and surface studies, respectively. However, depending on the application either the f_1 or f_2 modes can be set to the desired Larmor frequency.

2.3. S_{21} response of the RF assembly

The isolation S_{21} between the TX and RX was measured with the apparatus of Fig. 2. Fig. 5 shows a typical S_{21} response measured between the TX and RX_S coils (single-channel), in the presence of the RX_R coil connected to a 50 Ω load. The measured isolation for both peaks ($f_1 = 97.94$ MHz and $f_2 = 101.85$ MHz) was very poor (about −10 dB). Similar S_{21} results (not shown) were obtained between the TX and RX_R coils. It is worth noting that, as shown in Fig. 2, a 50 Ω load was connected to the RX_R (or the RX_S) coil when measuring the S_{21} response in single-channel mode.

Despite the strong coupling between the TX surface coil and each of the RX surface coils, it is possible to obtain a high degree of isolation between the TX and RX assembly. This is achieved with the double-channel RX configuration (Fig. 2) by adjusting the phase-shift/attenuation values in "subtraction" mode (phase shift = 180°, attenuation = 1 dB). It is worth noting that, with the current apparatus we are able to account for the *asymmetric* splitting of the resonant modes (f_1 and f_2) around f_0. In fact, the attenuation/phase-shift values of the auxiliary RX_R channel can be carefully adjusted to achieve high isolation at the Larmor frequency f_1 or f_2. Fig. 6A shows the measured S_{21} response of the RF assembly in subtraction mode and with the phase-shifter/attenuator values adjusted to obtain the best isolation (about −75 dB) at f_1; in this condition the isolation at f_2 showed a peak of about −23 dB. Fig. 6B shows the subtraction mode with the best isolation (about −78 dB) at the higher frequency f_2; in this condition the isolation at f_1 showed a peak of about −25 dB.

We have also investigated the effect of asymmetric positioning of the RX coils, with respect to the TX coil, on the S_{21} response when operating in subtraction mode. By positioning the RX_R and RX_S coils at $d_{cc} = 8$ cm and $d_{cc} = 13$ cm, respectively, we observed two resonant

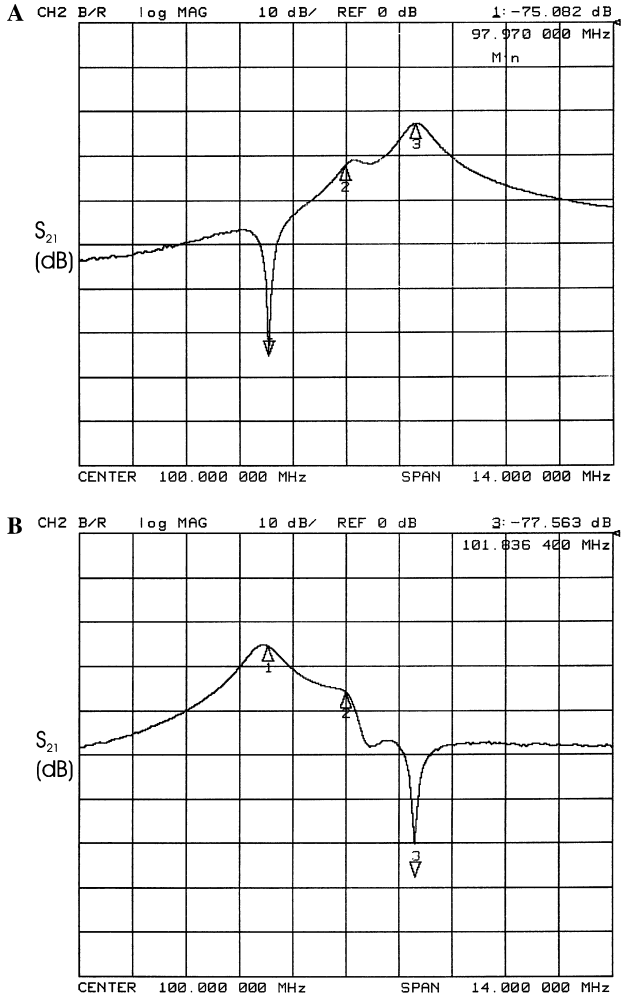

Fig. 6. S_{21} response (isolation) of the RF assembly in subtraction mode and with the phase-shifter/attenuator values adjusted to obtain the best isolation at: (A) $f_1 = 97.94$ MHz (S_{21} about -75 dB); and (B) $f_2 = 101.85$ MHz (S_{21} about -78 dB). The optimisation of the isolation at f_1 or f_2 is achieved by a fine adjustment of the phase-shift ($\pm 5°$) and attenuation (± 1 dB) values in the auxiliary RX channel.

peaks at $f_1 = 99.19$ MHz and $f_2 = 101.85$ MHz. In this condition, the measured isolation was about -50 dB. With the two RX coils positioned symmetrically at $d_{cc} = 6.0$ cm, the measured isolation was about -78 dB. These preliminary results show that the optimisation of the isolation requires a careful choice of the RF assembly geometrical parameter d_{cc}.

2.4. Dead time measurements

Fig. 7 shows a typical example of the RF pulse decay measured at the output of the single-channel RX (RX_S or RX_R coils) and the double-channel RX in subtraction mode. The TX pulse (duration 5 μs and amplitude 1500 mV) was tuned to the lower frequency f_1. The decay of the RF pulse was exponential with a time constant of about 510 ns with single-channel RX coil (RX_S or RX_R). In this condition the maximum RX output voltage was about 408 mV, with a resulting isolation between TX and single-channel RX of about -11 dB. This isolation value is comparable with the one measured in CW mode. With the double-channel RX in subtraction mode the decay of the RF pulse was exponential, with a slightly longer time constant (about 630 ns). The measured maximum RX output voltage (about 7 mV) was reduced by a factor 58. This corresponds to an isolation between TX and double-channel RX of about -47 dB. These results show that with the RF assembly in subtraction mode it is possible to increase the isolation of at least 36 dB. This isolation improvement corresponds to a significant reduction of the dead time. Similar results were obtained with the RF pulse frequency selected to f_2 and also with shorter (500 ns) RF pulses.

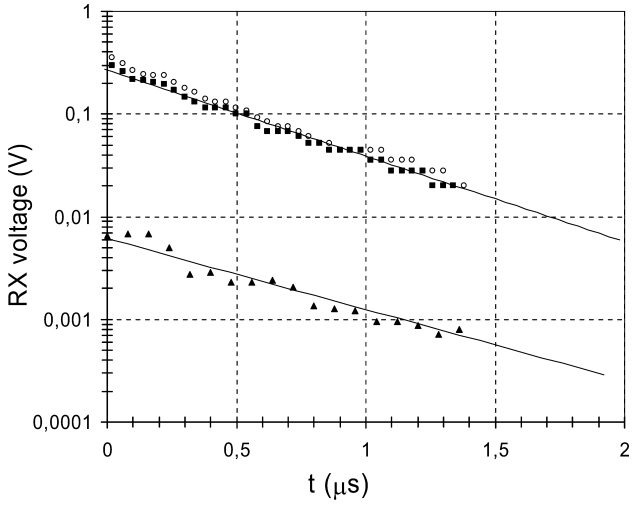

Fig. 7. An example of the RF pulse exponential decay measured at $f_1 = 97.94$ MHz with an apparatus comprising a RF source (HP8640B), gated by a pulse generator (Tabor Electronics, Model 8600), and connected via a directional coupler (Meca, Model 715-10-1) to the TX RF coil. A high frequency oscilloscope (Tektronix TDS520B) was used to record the RX voltage output of: (squares) the single-channel RX_S coil (max amplitude 372 mV, $\tau = 504$ ns); (circles) the single-channel RX_R coil (max amplitude 432 mV, $\tau = 518$ ns); (triangles) the double-channel RX in subtraction mode (max amplitude 7 mV, $\tau = 630$ ns). The time zero corresponds to the end of the TX RF pulse (duration 5 μs, amplitude 1500 mV). The lines represent the best fit of the measured data. Similar results (not shown) were obtained with the RF pulse frequency selected to $f_2 = 101.85$ MHz.

3. Conclusions

We have presented a novel open volume, high isolation, TX/RX RF assembly comprising a set of three circular loop RF surface coils (diameter 5.5 cm, $d_{cc} = 6.5$ cm) positioned with mutually parallel RF fields. Results obtained with a prototype operating at about 100 MHz are reported. These geometrical parameters and operating

frequency were selected as a reference model for potential applications of the RF assembly in solid state NMR [3] and in vivo EPR spectroscopy/imaging [5]. However, we anticipate that the RF assembly would be suited for a broader range of geometrical dimensions and operating frequencies. The circular loop geometry of the RF coil was chosen for easy of operation, but the dead time reduction would be effective with arbitrary RF coil geometry (e.g., square or rectangular loop). The RF apparatus permits the use of RF surface coils, allows an open volume access for the sample, and achieves high isolation at the Larmor frequency.

Theoretical and experimental RF B_1 mapping showed that: the lower frequency f_1 mode exhibits a good RF field homogeneity, with the B_{1x} variation less than 20% in a central region of about 3.5 cm; on the contrary, the higher frequency f_2 mode exhibits a large RF inhomogeneity with a minimum B_{1x} amplitude at about 3 cm from the TX coil. The RF field distribution of the f_1 and f_2 modes suggests that they are more suitable for volume and surface studies, respectively. However, depending on the application either the f_1 or f_2 modes can be set to the desired Larmor frequency.

Following a TX RF pulse (5 μs duration) we observed an exponential decay with a time constant of about 600 ns. The measured isolation between TX and single-channel RX coil was about −11 dB and it increased to about −47 dB with the double-channel RX in subtraction mode. These results show that with the RF assembly in subtraction mode it is possible to increase the isolation of at least 36 dB. This isolation improvement corresponds to a significant reduction of the dead time. Similar results were obtained with RF pulse frequency selected to f_2 and also with shorter (500 ns) RF pulses. Preliminary results show, that in pulsed mode, the isolation between the TX and double-channel RX can be further improved (up to −60 dB) by adjusting the position of the RX_R coil and/or the tuning frequency offset of the RX_S and RX_R coils with respect to the TX coil. The isolation results reported here are similar to that obtained with the RF assembly composed by three perpendicular RF coils [17]. In conclusion, the double-channel RF assembly should be well suited for the detection of MR signals of substances with very-short relaxation times (less than 100 μs).

References

[1] G.R. Davies, D.J. Lurie, J.M.S. Hutchinson, S.J. McCallum, I. Nicholson, Continuous-wave magnetic resonance imaging of short T2 materials, J. Magn. Reson. 148 (2001) 289–297.
[2] D.J. Lurie, S.J. McCallum, J.M.S. Hutchison, M. Alecci, Magnetic Resonance Imaging, USP 6,133,733 (2000).
[3] A.J. Fagan, G.R. Davies, J.M.S. Hutchinson, D.J. Lurie, Continuous wave MRI of heterogeneous materials, J. Magn. Reson. 163 (2003) 318–324.
[4] J.H. Strange, M.R. Hales, Imaging techniques for solids and quasi-solids, in: D.M. Grant, R.K. Harris (Eds.), The Encyclopaedia of Nuclear Magnetic Resonance, Wiley, New York, 1995, pp. 2472–2481.
[5] M. Alecci, J. Brivati, G. Placidi, A. Sotgiu, A radiofrequency (220 MHz) Fourier Transform EPR spectrometer, J. Magn. Res. 130 (1998) 272–280.
[6] G.A. Rinard, R.W. Quine, G.R. Eaton, An L-band crossed-loop (bimodal) EPR resonator, J. Magn. Reson. 144 (2000) 85–88.
[7] S. Subramanian, N. Devasahayam, R. Murugesan, K. Yamada, J. Cook, A. Taube, J.B. Mitchell, J.A. Lohman, M.C. Krishna, Single-point (constant-time) imaging in radiofrequency Fourier transform electron paramagnetic resonance, Magn. Reson. Med. 48 (2002) 370–379.
[8] K. Yamada, R. Murugesan, N. Devasahayam, J.A. Cook, J.B. Mitchell, S. Subramanian, M.C. Krishna, Evaluation and comparison of pulsed and continuous wave radiofrequency electron paramagnetic resonance techniques for in vivo detection and imaging of free radicals, J. Magn. Reson. 154 (2002) 287–297.
[9] P. Mansfield, J.G. Powles, A microsecond nuclear resonance pulse apparatus, J. Sci. Instrum. 40 (1963) 232–238.
[10] R.E. Amen, Pulsed resonance spectrometer system employing improved radio frequency pulse turn-off method and apparatus, USP 3,768,003 (1973).
[11] M. Savelainen, Measuring procedure for the elimination of faults from an NMR signal by comparing RF field components spinning in opposite directions, USP 5,068,611 (1991).
[12] M.I. Hrovat, S. Patz, Pulse sequence for elimination of RF receiver coil ringing down, Proc. Int. Soc. Magn. Reson Med. 9 (2001) 914.
[13] M. Alecci, J. Brivati, G. Placidi, L. Testa, D.J. Lurie, A. Sotgiu, A submicrosecond resonator and receiver system for pulsed magnetic resonance with large samples, J. Magn. Res. 132 (1998) 162–166.
[14] M. Alecci, J. Brivati, G. Placidi, L. Testa, A. Sotgiu, D.J. Lurie, Magnetic resonance apparatus having reduced dead time, USP 6,150,817 (2000).
[15] M. Alecci, G. Placidi, D.J. Lurie, A. Sotgiu, Theoretical and experimental optimisation of the dead time of RF coils, Proc. Int. Soc. Magn. Reson. Med. 8 (2001) 1401.
[16] C.A. Curto, G. Placidi, A. Sotgiu, M. Alecci, Disposizione di rilevamento per una apparecchiatura per risonanza magnetica di tipo perfezionato, ed apparecchiatura per risonanza magnetica comprendente una tale disposizione, Italian Patent TO2003A000465, 19 June (2003).
[17] C.A. Curto, G. Placidi, A. Sotgiu, M. Alecci, Design and testing of a high isolation radio frequency receiver system for pulsed magnetic resonance imaging, Book of Abstracts, European Society for Magnetic Resonance in Medicine and Biology, 20th Annual Scientific Meeting, Rotterdam, September 18–21 (2003).
[18] F.W. Grover, Inductance Calculation, Dover, New York, 1973.
[19] C.N. Chen, D.I. Hoult, Biomagnetic Magnetic Resonance Technology, IOP Publishing, Bristol, 1989.
[20] F.E. Terman, Radio Engineering, McGraw-Hill, New York, 1937.
[21] R. Diodato, M. Alecci, J. Brivati, A. Sotgiu, Resonant inductive coupling of RF EPR resonators in the presence of electrically conducting samples, Meas. Sci. Technol. 9 (1998) 832–837.